Maternal Diabetes Compromises the Organization of Hypothalamic Feeding Circuits and Impairs Leptin Sensitivity in Offspring

Sophie M. Steculorum and Sebastien G. Bouret

The Saban Research Institute (S.M.S., S.G.B.), Neuroscience Program, Children's Hospital Los Angeles, University of Southern California, Los Angeles, California 90027; and Institut National de la Santé et de la Recherche Médicale, Jean-Pierre Aubert Research Center, Unité 837, University Lille 2, Lille 59045, France

Maternal diabetes is a common complication of pregnancy, and the offspring of diabetic mothers have a higher risk of developing obesity and type 2 diabetes later in life. Despite these observations, the precise biological processes mediating this metabolic programming are not well understood. Here, we explored the consequences of maternal diabetes on the organization of hypothalamic neural circuits involved in the regulation of energy balance. To accomplish this aim, we used a mouse model of maternal insulin deficiency induced by streptozotocin injections. Maternal diabetes was found to be associated with changes in offspring growth as revealed by a significantly higher pre- and postweaning body weight in the offspring of insulin-deficient dams relative to those of control mice. Mice born to diabetic dams also showed increased fasting glucose levels, increased insulin levels, and increased food intake during their adult lives. These impairments in metabolic regulation were associated with leptin resistance during adulthood. Importantly, the ability of leptin to activate intracellular signaling in arcuate neurons was also significantly reduced in neonates born to diabetic dams. Furthermore, neural projections from the arcuate nucleus to the paraventricular nucleus were markedly reduced in the offspring of insulin-deficient dams. Together, these data show that insulin deficiency during gestation has long-term consequences for metabolic regulation. They also indicate that animals born to diabetic dams display abnormally organized hypothalamic feeding pathways that could result from the attenuated responsiveness of hypothalamic neurons to the neurotrophic actions of leptin during neonatal development. (*Endocrinology* 152: 4171–4179, 2011)

Abnormal maternal glucose regulation occurs in 3–10% of pregnancies (1). In addition to adversely affecting the health of the mother, epidemiological and animal studies indicate that maternal diabetes has deleterious health effects on offspring (2). Remarkably, insulin deficiency (type 1 diabetes mellitus) and insulin excess (type 2 diabetes mellitus) during pregnancy both increase the risk that offspring will develop obesity and type 2 diabetes (3–5). These observations provide evidence that a balanced perinatal hormonal environment is an important determinant of future weight gain, adiposity, and other physiological properties.

The signals that mediate the effects of maternal metabolic disorders in offspring have not been identified, but hormones, such as insulin and leptin, and nutrients, such as glucose, may influence perinatal development. For example, maternal hyperglycemia (induced by either insulin deficiency or insulin resistance) is associated with fetal and early postnatal hyperglycemia, which in turn may cause elevations in perinatal insulin levels, leading to an increase

Abbreviations: AgRP, Agouti-related peptide; ARH, arcuate nucleus of the hypothalamus; G, gestation day; αMSH, α-melanocyte-stimulating hormone; NPY, neuropeptide Y; P, postnatal day; POMC, proopiomelanocortin; pSTAT3, phosphorylated form of the signal transducer and activator of transcription 3; PVH, paraventricular nucleus of the hypothalamus; STZ, streptozotocin; WAT, white adipose tissue.

in fetal growth and adiposity (6, 7). Thus, an abundance of evidence suggests that alterations in the perinatal hormonal environment and subsequent postnatal growth can predispose an individual to obesity and diabetes. Studies that have investigated the possible mechanisms mediating this disturbance in metabolic regulation have largely focused on peripheral measures and outcomes (see Ref. 8). Nevertheless, a growing body of evidence suggests that developmental programming of neuroendocrine systems by the perinatal environment could cause these diseases.

Appetite and energy expenditure are carefully regulated by a complex neuronal network (for review, please see Refs. 9–11). The important components of this network include neurons located in the arcuate nucleus of the hypothalamus (ARH) and particularly neurons producing proopiomelanocortin (POMC) and neuropeptide Y (NPY)/agouti-related peptide (AgRP). Each of these neuronal populations provides overlapping projections to other key parts of the hypothalamus, including the paraventricular nucleus of the hypothalamus (PVH), exerting opposing effects on appetite regulation. POMC neurons represent important anorectic regulators and NPY/AgRP neurons act as major orexigenic signals.

ARH neural circuits involved in appetite regulation develop primarily during the first 3 wk of postnatal life in rodents (12–14) under the control of both genetic and environmental factors. In particular, experiments carried out in leptin-deficient mice have provided compelling evidence that leptin is required for the proper development of ARH projections through direct action on the brain (15). Importantly, the developmental actions of leptin also appear to contribute to the ultimate phenotype of the organism (15–17), suggesting the importance of leptin-regulated arcuate circuit formation to future energy balance.

Although perinatal hormones appear to be important determinants of optimal physiological regulation, the precise neurobiological mechanisms that contribute to the programming effects of hormones are not well understood. In the present study, we used a commonly used and well-described rodent model of insulin-deficient diabetes induced by streptozotocin (STZ) injections (18–24) to determine whether changes in maternal insulin levels during a critical period of development influence leptin sensitivity in progeny and have enduring consequences on the organization of appetite-regulating hypothalamic neural circuits.

Materials and Methods

Animals

Adult C57BL/6 mice (Charles River, L'Arbresle, France) were housed in individual cages under specific pathogen-free condi-

tions, maintained in a temperature-controlled room with a 12-h light, 12-h dark cycle, and provided *ad libitum* access to water and standard laboratory chow (Special Diet Services, Commenailles, France). The protocols used here were approved by the Institut National de la Santé et de la Recherche Médicale guidelines for the Care and Use of Laboratory Animals. The animals used and experiments conducted in this study were in accordance with the European Communities Council Directive of November 24th, 1986 (86/609/EEC) regarding mammalian research. Only male offspring were studied.

Induction of maternal insulin-deficient diabetes by STZ injection

This study used a mouse model of maternal insulin deficiency induced by STZ injections. STZ is a pancreatic β-cell toxin that is widely used to experimentally manipulate insulin levels (19–24). Adult female mice were mated with males and checked for a vaginal plug the next day [gestation day (G)0.5]. On G5.5, pregnant females (n = 6) received a single ip injection of freshly prepared STZ (200 mg/kg; Sigma, Saint-Quentin Fallavier, France) dissolved in ice-cold 50 mM sodium citrate (pH 4.5). An additional group of mice (n = 6) received vehicle injections [50 mM sodium citrate (pH 4.5)]. The rationale for injecting STZ at G5.5 was primarily to prevent the occurrence of anovulation and miscarriages that are often observed when diabetes is induced just before or at conception (*i.e.* before embryo implantation). Maternal glycemia was assessed during pregnancy by testing tail blood samples with a glucometer (One Touch Ultra; Johnson & Johnson, Issy-les-Moulineaux, France). Three litters per group were used for neonatal studies, and three separate litters per group were used for adult studies.

Insulin immunohistochemistry and analysis

Twenty-two days after parturition (weaning), dams (n = 4 per group) were anesthetized and perfused transcardially with 4% paraformaldehyde. Pancreases were frozen, sectioned, and then processed for immunostaining. Briefly, sections were incubated overnight in a guinea pig antiinsulin antibody (1:50; Abcam, Paris, France). The primary antibody was detected with horseradish peroxidase-conjugated goat antiguinea pig IgG (1:200; Millipore, Molsheim, France). Horseradish peroxidase was revealed using 3,3′-diaminobenzidine. Sections were then counterstained using hematoxylin to visualize cell nuclei and coverslipped with buffered glycerol (pH 8.5). For quantification, images were acquired through the pancreases (four sections per animal) of the animals of each group using a Zeiss Axio Imager Z1 microscope equipped with a ×20 objective (Zeiss, Jena, Germany). Total cells per islet and insulin-IR cells per islet were quantified using ImageJ software (ImageJ 1.39 T; National Institutes of Health, Bethesda, MD). The average number of cells counted from four islets in each mouse was used for statistical comparisons.

Physiological measures

One day after birth, the litter size was adjusted to six pups (three males and three females) to ensure adequate and standardized nutrition until weaning. The body weights of male offspring of STZ-treated dams (n = 7 males from three litters) and vehicle-treated dams (n = 9 males from three litters) were measured at postnatal days (P)2, P6, P10, P14, P18, and P22 (wean-

ing) and P63, P70, P80, and P120 (adults) using an analytical balance. To measure food consumption, P90 mice were housed individually in cages, and food intake was measured every 24 h for 3 d from preweighed portions of food dispensed from wire cage tops. The average daily food intake of each mouse was used for statistical comparisons. Glucose levels were assessed in adult (P70) mice after overnight fasting, using a glucometer (One Touch Ultra; Johnson & Johnson).

Histomorphological assessment of white adipose tissue (WAT)

Male offspring of STZ-treated dams (n = 7 males from three litters) and vehicle-treated dams (n = 9 males from three litters) were anesthetized at P120 of age and perfused transcardially with 4% paraformaldehyde. Epididymal adipose tissue was frozen, sectioned at 10 μm, and stained with hematoxylin and eosin. Sections were imaged using a Leica microscope (DMRB) (Leica, Nanterre, France) equipped with a Leica camera interface (DC 300FX) with a $\times$20 objective. Adipocyte diameter was calculated using ImageJ software (ImageJ 1.39 T; National Institutes of Health). The average adipocyte size measured from five sections in each mouse was used for statistical comparisons.

Serum leptin and insulin levels

Serum leptin and insulin levels were characterized in the two experimental groups of mice by collecting tail blood samples from P90 male offspring of STZ-treated dams (n = 7 males from three litters) and vehicle-treated dams (n = 9 males from three litters). Additionally, serum insulin levels were measured in dams by collecting tail blood samples from STZ- and vehicle-treated dams 10 d after STZ or vehicle treatment. Leptin and insulin levels in the plasma samples were assayed for leptin and insulin using multiplex technology (Millipore) with the assistance of the Assay and Analytical Core Service in the Keck School of Medicine of the University of Southern California.

In vivo leptin sensitivity test

Adult (P80) male offspring of STZ- (n = 7 males from three litters) and vehicle-treated dams (n = 9 males from three litters) were injected ip at 0800 and 1630 h with vehicle [5 mM sodium citrate buffer (pH 4.0)] or leptin (1 mg/kg; PeproTech, Neuilly-sur-Seine, France), according to the following scheme: vehicle injections for 1 d followed by leptin injections for 1 d. Animals were weighed daily during the injection period. Animals were allowed to recover for 10 d after the last injection and were kept for further studies.

Phosphorylated form of the signal transducer and activator of transcription 3 (pSTAT3) immunostaining and analysis

P10 male offspring of STZ- and vehicle-treated dams were injected ip with either leptin (10 mg/kg; PeproTech) or vehicle alone [5 mM sodium citrate buffer (pH 4.0)] (n = 4 males from three litters for each group) and were perfused 45 min later with a solution of 2% paraformaldehyde. Frozen coronal sections were cut at 30 μm and then processed for pSTAT3 immunostaining as described previously (25, 26). For quantification, images were acquired through the arcuate nucleus of the animals of each group using a Zeiss Axio Imager Z1 apotome micro-

scope equipped with a $\times$20 objective. pSTAT3 immunopositive cells in the ARH were manually counted using ImageJ software (ImageJ 1.39 T; National Institutes of Health). The average number of cells counted in two ARH sections in each mouse was taken for statistical comparisons.

AgRP and α-melanocyte-stimulating hormone (αMSH) immunostaining and analysis

Adult male mice of STZ-treated dams (n = 7 males from three litters) and vehicle-treated dams (n = 9 males from three litters) were anesthetized and perfused transcardially at P120 with 4% paraformaldehyde, and then the brains were frozen and sectioned at 30 μm and processed for immunofluorescence as described elsewhere (15, 25). Briefly, sections were incubated with rabbit anti-AgRP (1:4000; Phoenix Pharmaceuticals, Strasbourg, France) or sheep anti-αMSH (1:40,000; Millipore). The primary antibodies were detected with Alexa Fluor 488 goat antirabbit IgG or Alexa Fluor 568 donkey antisheep IgG (1:200; Invitrogen, Villebon-sur-Yvette, France). Sections were counterstained using bis-benzamide (1:3000; Invitrogen) to visualize cell nuclei and then coverslipped with buffered glycerol (pH 8.5). For quantification, images were acquired through the PVH (two sections per animal) of the animals in each group using a Zeiss Axio Imager Z1 apotome microscope equipped with a $\times$20 objective. Image analysis was performed using ImageJ software (ImageJ 1.39 T; National Institutes of Health), as described previously (14, 15, 25). Briefly, each picture was binarized. The integrated density was then calculated for each image, which is a figure that reflects the total number of pixels in the binarized image and is proportional to the total density of labeled fibers in the image. The average integrated density measurement in two PVH sections in each animal was used for statistical comparisons. For quantification of cell numbers, animals were perfused at P10 (n = 4 males from three litters for each group) with 2% paraformaldehyde, and brains sections were processed for immunofluorescence as described above. Images were acquired through the arcuate nucleus of the animals of each group, and αMSH- and AgRP-immunopositive cells in the ARH were manually counted using ImageJ software (ImageJ 1.39 T; National Institutes of Health). The average number of cells counted in two ARH sections in each mouse was taken for statistical comparisons.

Statistical analysis

Data are presented as the mean $\pm$ SEM. When more than one animal was used in the litter, values for littermates were averaged, and the mean data for each litter were used for the statistical analysis. Statistical analyses were carried out with Sigma Stat software (Statistical software 2.0). Before statistical analysis, percentages were subjected to arc-sine transformation to convert them from binomial to normal distributions. The data were analyzed with Student's t test. The statistical significance of differences in body weight was analyzed using two-way ANOVA. $P < 0.05$ indicated statistical significance.

Results

Induction of insulin-deficient diabetes during pregnancy

To explore the consequences of maternal diabetes during pregnancy in the offspring, we used a previously de-
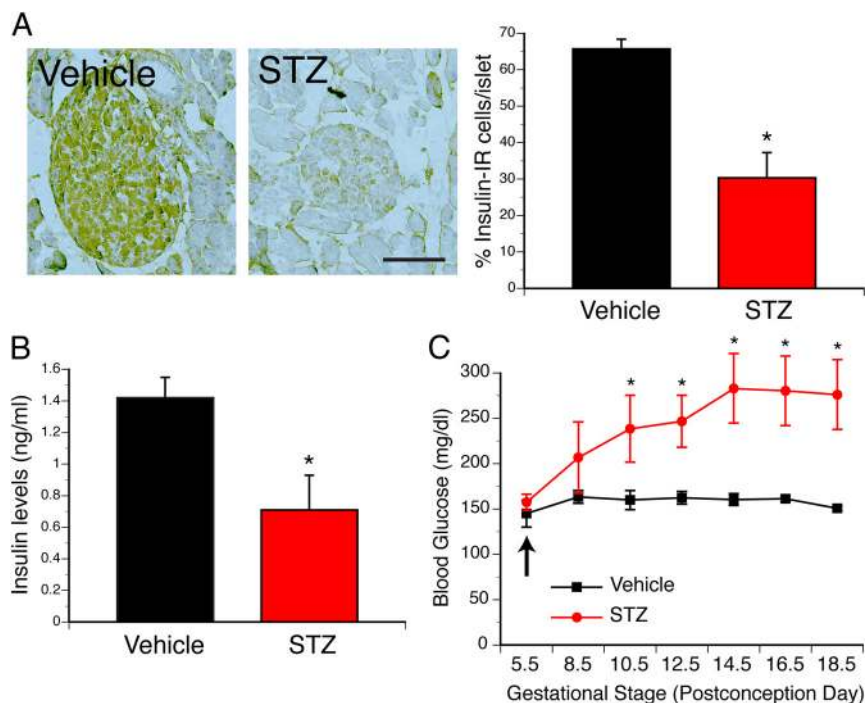
FIG. 1. STZ injection during gestation induces insulin-deficient diabetes mellitus. A, Microphotographs and quantification of insulin-immunoreactive cells (*brown* precipitate) in the pancreatic islets of dams injected with vehicle or STZ. B, Plasma insulin levels in pregnant dams 10 d after injection of vehicle or STZ. C, Maternal blood glucose levels in dams injected with vehicle or STZ at G5.5. The values shown are means ± SEM; *, $P < 0.05$ between vehicle and STZ (n = 4 dams per group). *Scale bar*, 320 μm.

veloped animal model of insulin-deficient diabetes induced by STZ injection (19–24). As expected, given the established ability of STZ to destroy β-cells, STZ-treated dams displayed a 2-fold decrease in insulin-immunoreactive cells in pancreatic islets compared with vehicle-treated animals (Fig. 1A). A 2-fold decrease in serum insulin levels was also observed in STZ-treated dams compared with vehicle-treated animals (Fig. 1B). Consistent with these observations, a single STZ injection induced a marked increase in blood glucose levels that began 3 d after injection and became significantly different 5 d after injection. Importantly, the elevated levels of glucose observed in STZ-treated dams persisted throughout gestation (Fig. 1C). In contrast, vehicle-treated animals did not show any changes in blood glucose levels throughout pregnancy (Fig. 1C). Importantly, a dramatic induction of cell death was exclusively observed in Langerhans islets of STZ-treated dams (Supplemental Fig. 1, published on The Endocrine Society's Journals Online web site at http://endo.endojournals.org). However, there were no noticeable differences in cell death between fetuses of STZ- and vehicle-treated dams (Supplemental Fig. 1), indicating that STZ selectively destroys β-cells of dams and does not disrupt organogenesis in the fetuses.

Consequences of maternal diabetes on metabolic regulation in offspring

We then used this animal model to study the impact of maternal diabetes during gestation on the offspring's metabolism. Induction of diabetes during gestation was associated with changes in offspring growth, as revealed by a significantly higher pre- and postweaning body weights in offspring born to STZ-injected dams compared with control animals (Fig. 2, A and B). Compared with control pups, STZ-derived pups had heavier body weights as early as P18 (Fig. 2A). STZ offspring remain heavier after weaning, and this elevated body weight persisted into adulthood (Fig 2B). This increase in body weight was also associated with an increase in food intake during adulthood (Fig. 2C). In addition, fasting blood glucose levels were also higher in adult animals born to diabetic dams compared with control mice (Fig. 2E). Furthermore, serum insulin levels were 1.5-fold higher in adult STZ offspring compared with control animals (Fig. 2F). Glucose- and insulin-tolerance tests would be necessary to determine the degree of impairment in glucose homeostasis in STZ offspring. Histomorphological analysis of epididymal WAT revealed a significant increase in the mean adipocyte size in adult mice born to STZ-treated animals compared with control animals (Fig. 2D). Similarly, serum leptin levels were 2-fold higher in adult STZ offspring compared with control animals (Fig. 3A). The increased adiposity and leptin levels observed in animals born to diabetic dams suggest the possibility that these animals acquired leptin resistance. Accordingly, we next investigated leptin sensitivity in animals born to diabetic dams and found that the ability of leptin to induce weight loss was attenuated in the adult offspring of STZ-treated dams, compared with control animals (Fig. 3B). However, whether the weight loss effects of leptin are mediated by changes in food intake remain to be investigated.

Altered central leptin signaling in pups born to diabetic mothers

Adult mice born to diabetic dams were found to exhibit evidence of leptin resistance, but whether neonates are similarly affected and whether this leptin resistance occurs at a central level remains unknown. To determine whether
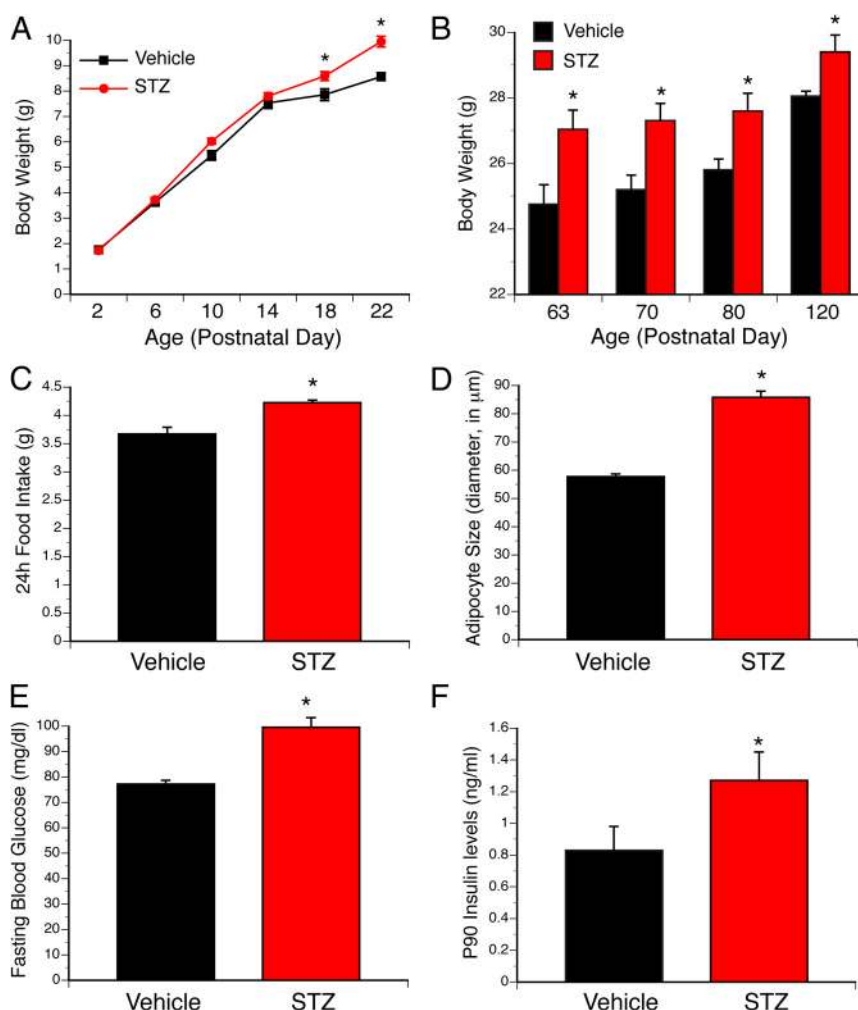
FIG. 2. Offspring born to diabetic dams display metabolic dysfunctions. A, Preweaning growth curves of pups born to control (vehicle) or diabetic (STZ) dams. B, Body weight of offspring of control (vehicle) or diabetic (STZ) dams at 63, 70, 80, and 120 d of age. C, Food intake of adult (P90) offspring born to control (vehicle) or diabetic (STZ) dams over 24 h. D, Quantification of mean adipocyte size in the epididymal WAT of adult (P120) mice born to control (vehicle) or diabetic (STZ) dams. E, Blood glucose levels in adult (P70) mice born to control (vehicle) or diabetic (STZ) dams. F, Plasma insulin levels in adult (P90) offspring of control (vehicle) and diabetic (STZ) dams. The values shown are means ± SEM; *, $P < 0.05$ between vehicle and STZ (n = 7 males from three litters and n = 9 males from three litters for the STZ and vehicle group, respectively).

the offspring of diabetic dams display impaired leptin signaling in the ARH, we next evaluated the number of pSTAT3-IR neurons in the ARH of P10 pups derived from diabetic and nondiabetic dams 45 min after ip injection with leptin. This approach is based on the fact that STAT3 is a key component of the intracellular signaling pathway downstream of the leptin receptor. Leptin treatment caused a marked increase in the number of pSTAT3-IR cells in the ARH of control pups (Fig. 4A). However, the same leptin treatment resulted in significantly fewer pSTAT3-IR cells in the ARH of pups born to diabetic dams (Fig. 4A). A quantitative analysis revealed that the number of pSTAT3-immunoreactive cells in the ARH of pups born to diabetic dams was reduced by more than 30% com-

pared with control mice (Fig. 4B). These results suggest that leptin signaling in ARH neurons is impaired during postnatal development in the offspring of diabetic dams.

Disrupted organization of hypothalamic neural projections in animals born to diabetic dams

Based on previous findings showing that alterations in leptin signaling during early life led to abnormal development of the hypothalamic circuits involved in energy balance (15, 25), we hypothesized that the changes in leptin sensitivity observed in the ARH of pups born to diabetic dams may impact the organization of their ARH neural projections. Therefore, we performed immunofluorescent labeling of AgRP and αMSH (two metabolically relevant neuropeptide systems produced by ARH neurons) in brain sections derived from adult offspring of diabetic and nondiabetic mice. The density of AgRP-IR fibers in the PVH of adult animals born to diabetic mice was half that observed in control animals (Fig. 5A). Similarly, a 2-fold reduction in the density of αMSH-immunoreactive fibers was observed in the PVH of animals born to diabetic dams compared with control mice (Fig. 5B). However, the overall distribution pattern of AgRP- and αMSH-labeled fibers in the PVH was similar between animals born to STZ- and vehicle-treated dams, suggesting that maternal diabetes alters the density but not the pattern of innerva-

tion. Also, a 1.3-fold increase in the number of αMSH-containing neurons was observed in the ARH of animals born to diabetic dams compared with control mice (Fig. 6B). However, the number of AgRP-containing neurons was identical between animals born to STZ- and vehicle-treated dams (Fig. 6A). These observations indicate that the low density of fibers is due to alterations in axon growth as opposed to a reduction in cell number.

Discussion

Circulating hormones are well established as important environmental signals that can act directly on the central
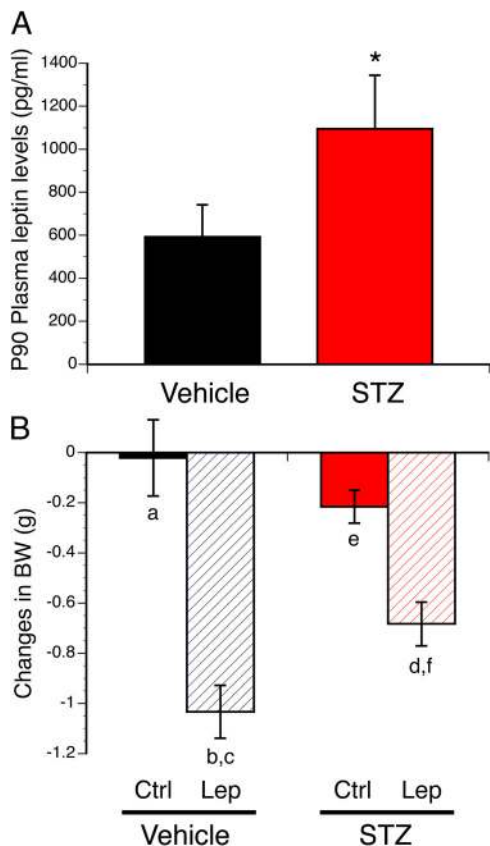
FIG. 3. Leptin resistance in animals born to diabetic dams. A, Plasma leptin levels in adult (P90) offspring of control (vehicle) and diabetic (STZ) dams. B, Body weight changes after ip administration of leptin (Lep) or vehicle (Ctrl) in adult (P80) offspring of vehicle- or STZ-treated dams over 24 h. The values shown are mean $\pm$ SEM; $P < 0.05$ between a and b; c and d; and e and f ($n = 7$ males from three litters and $n = 9$ males from three litters for the STZ and vehicle group, respectively).

FIG. 4. ARH neurons exhibit a reduced response to leptin in neonates born to diabetic dams. A and B, Photomicrographs (A) and quantification (B) of the number of pSTAT3 immunoreactive cells in the arcuate nucleus (ARH) of P10 pups born to diabetic (STZ) or nondiabetic (vehicle, Veh) dams, after ip administration of leptin (Lep) or vehicle (Ctrl). The values shown are mean $\pm$ SEM; $P < 0.05$ between * and ** ($n = 4$ males from three litters for each group). *Scale bar*, 120 μm.

nervous system to regulate its development and activity (27–29). However, the association between maternal insulin deficiency and the organization of hypothalamic appetite-related circuits has never been examined. The neuroanatomical experiments presented here indicate that animals born to insulin-deficient diabetic dams display structural alterations in the density of AgRP- and αMSH-immunoreactive fibers innervating the PVH. Importantly, these ARH neuropeptidergic projections to the PVH are known to play a particularly important role in energy balance regulation (for review, please see Refs. 9–11).

Using a similar animal model, Plagemann *et al.* (18, 30) and Plagemann and co-workers (31) previously reported that rat pups born to STZ-treated dams had an increased number of NPY- and galanin-containing neurons in the ARH. In our mouse model, we did not observed any difference in the number of AgRP neurons in the ARH of animals born to diabetic dams. However, the number of POMC neurons was increased in the ARH of pups born to STZ-treated dams compared with control mice. Consistent with these observations, using a mouse model of ma-
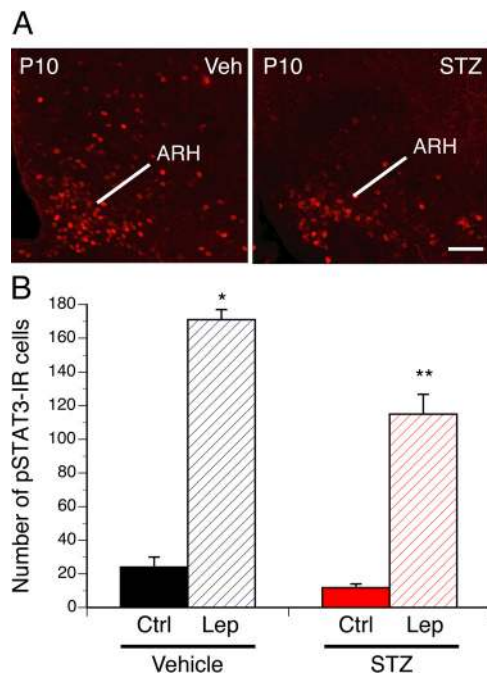
ternal insulin resistance, Carmody *et al.* (32) showed that maternal hyperinsulinemia is associated with an increased number of ARH POMC-expressing neurons in their offspring. These data suggest that maternal diabetes can influence developmental processes that specify cell numbers, such as neurogenesis, neuron migration, and cell death. Our data indicate that maternal diabetes causes more widespread structural alterations than was previously known, affecting not only hypothalamic cell numbers but also the density of neural projections involved in appetite regulation. Importantly, we found that despite an increase in ARH POMC neurons, pups born to diabetic dams display a reduction in αMSH fiber density in the PVH, suggesting that the low density of fibers is due to alterations in axon growth as opposed to a reduction in cell number.

The precise mechanisms responsible for the disruption in ARH projections remain to be determined. However, the attenuation in leptin signaling observed in the ARH of pups born to STZ dams represents a plausible cause for the perturbed development of ARH projections. Previous studies demonstrated that altered leptin signaling during critical postnatal periods is associated with disrupted development of ARH projections (15, 25). Notably, we report here that neonates born to insulin-deficient dams have altered leptin-induced pSTAT3 levels in the ARH at
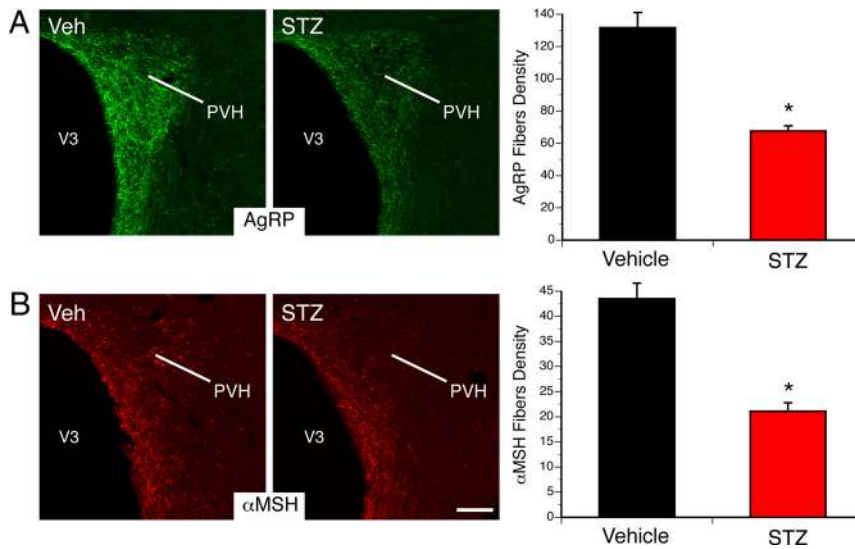
FIG. 5. Altered AgRP and αMSH neural projections in adult (P120) offspring of diabetic dams. A and B, Microphotographs and quantification of AgRP (A) and αMSH (B) immunoreactive fibers innervating the paraventricular nucleus (PVH) in adult animals born to control (vehicle, Veh) or diabetic (STZ) dams. V3, Third ventricle. The values shown are mean ± SEM; *, $P < 0.05$ between vehicle and STZ (n = 7 males from thee litters and n = 9 males from three litters for the STZ and vehicle group, respectively). *Scale bar*, 130 μm.

the time when ARH projections develop and before they become overweight (14). Therefore, suppressed leptin signaling in ARH neurons of pups born to diabetic dams could contribute to the perturbation of ARH projections. Equally important would be to measure leptin levels in pups born to STZ dams to determine whether changes in neonatal leptin levels could also contribute to early leptin resistance and disruption of ARH neural projections. Re-

markably, leptin resistance is also found in the adult offspring of diabetic dams despite exposure to a healthy standard diet. Whether this leptin resistance is also associated with increased fat mass remains to be investigated. In addition to leptin signaling, changes in other developmental signals could also contribute to these alterations of ARH projections. For example, insulin has long been associated with brain development, and pups born to diabetic and hyperglycemic mothers display compensatory hyperinsulinemia that may cause neurodevelopmental defects (6, 7). Consistent with this idea, direct injection of insulin to the region of the mediobasal hypothalamus in the immediate postnatal period recapitulates most of the metabolic and structural abnormalities found in pups born to insulin-deficient dams (18, 33). Although the precise biological mechanisms responsible for the structural defects observed in pups born to diabetic dams remain to be determined, these data suggest that correct insulin levels and/or leptin signaling during early postnatal life may be important determinants for proper hypothalamic development.

Previous studies have demonstrated that animals born to diet-induced obese dams also display abnormally organized hypothalamic feeding pathways (34). Although these results indicate that maternal obesity plays an important role in neonatal development, they do not address the specific role that it plays. Indeed, prolonged high-fat feeding in rodents also causes diabetes, which likely acts in concert with obesity to influence the development of offspring. By examining the influence of maternal diabetes independently of obesity, the present study showed that maternal diabetes alone can cause early central leptin resistance with enduring consequences for the organization of hypothalamic pathways involved in appetite regulation. Intriguingly, both maternal insulin-deficient diabetes and maternal noninsulin-dependent diabetes are associated with similar metabolic outcomes, including overweight status and impaired glucose
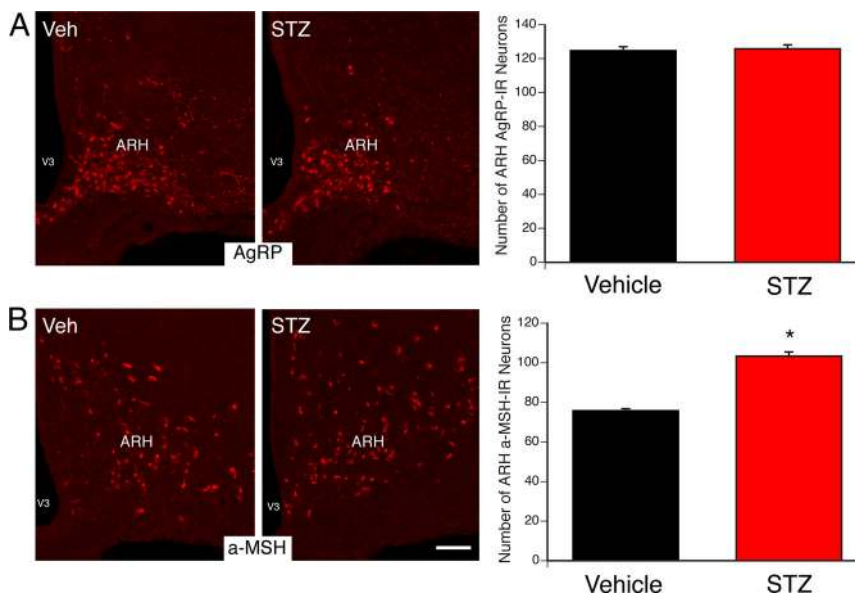

FIG. 6. Increased number of POMC neurons in the arcuate nucleus of animals born to diabetic dams. A and B, Microphotographs and quantification of AgRP (A) and αMSH (B) cell numbers in the arcuate nucleus (ARH) of P10 animals born to control (vehicle, Veh) or diabetic (STZ) dams. V3, Third ventricle. The values shown are mean ± SEM; *, $P < 0.05$ between vehicle and STZ (n = 4 males from three litters for each group). *Scale bar*, 120 μm.

homeostasis (18, 30–32). This observation suggests that the programmed metabolic dysregulation observed in these individuals may be tied to the same biological mechanism. An early hormonal imbalance can have adverse effects on the development of various organs, thereby exerting an enduring impact on the metabolic status of progeny (19, 27, 35, 36). For example, maternal insulin deficiency and insulin resistance can disrupt the development of the pancreatic islets, adipose tissue, and the intestine, each of which plays a key role in metabolic regulation (37–39). It is also likely that the structural alterations found in the metabolic hypothalamus of animals born to either insulin-deficient dams (the present study and Refs. 18, 30, 31) or insulin-resistant dams (32) may contribute to the development of metabolic dysfunction. However, it is clear that there are also marked metabolic differences between type 1 and type 2 diabetes, including lipid and cytokine profiles, and future work will be required to address how maternal type 2 diabetes may, independently of obesity, impact developmental events.

In conclusion, these experiments show that maternal insulin-deficient diabetes results in early hypothalamic leptin resistance and is associated with lifelong disorganization of the hypothalamic pathways that control feeding and energy balance. These findings also support the emerging concept that changes in the perinatal hormonal environment during this critical period of development can have permanent structural effects that may contribute to the development of diseases later in life.

Acknowledgments

References

1. **Anna V, van der Ploeg HP, Cheung NW, Huxley RR, Bauman AE** 2008 Sociodemographic correlates of the increasing trend in prevalence of gestational diabetes mellitus in a large population of women between 1995 and 2005. Diabetes Care 31:2288–2293

2. **Whitaker RC, Pepe MS, Seidel KD, Wright JA, Knopp RH** 1998 Gestational diabetes and the risk of offspring obesity. Pediatrics 101:e9

3. **Silverman BL, Metzger BE, Cho NH, Loeb CA** 1995 Impaired glucose tolerance in adolescent offspring of diabetic mothers. Relationship to fetal hyperinsulinism. Diabetes Care 18:611–617

4. **Pettitt DJ, Aleck KA, Baird HR, Carraher MJ, Bennett PH, Knowler WC** 1988 Congenital susceptibility to NIDDM. Role of intrauterine environment. Diabetes 37:622–628

5. **Berenson GS, Bao W, Srinivasan SR** 1996 Abnormal characteristics of young offspring of parents with noninsulin-dependent diabetes mellitus. The Bogalusa heart study. Am J Epidemiol 144:962–967

6. **Pedersen J** 1952 Diabetes and pregnancy: blood sugar of newborn infants. Copenhagen: Danish Science Press; 230

7. **Pedersen J** 1967 Pathogenesis of the characteristic features of newborn infants of diabetic women. In: The pregnant diabetic and her newborn: problems and management. Baltimore: William & Wilkins; 128–137

8. **McMillen IC, Adam CL, Mühlhäusler BS** 2005 Early origins of obesity: programming the appetite regulatory system. J Physiol 565: 9–17

9. **Elmquist JK, Coppari R, Balthasar N, Ichinose M, Lowell BB** 2005 Identifying hypothalamic pathways controlling food intake, body weight, and glucose homeostasis. J Comp Neurol 493:63–71

10. **Schwartz MW, Woods SC, Porte Jr D, Seeley RJ, Baskin DG** 2000 Central nervous system control of food intake. Nature 404:661–671

11. **Sawchenko PE** 1998 Toward a new neurobiology of energy balance, appetite, and obesity: the anatomists weigh in. J Comp Neurol 402: 435–441

12. **Grove KL, Allen S, Grayson BE, Smith MS** 2003 Postnatal development of the hypothalamic neuropeptide Y system. Neuroscience 116:393–406

13. **Nilsson I, Johansen JE, Schalling M, Hokfelt T, Fetissov SO** 2005 Maturation of the hypothalamic arcuate agouti-related protein system during postnatal development in the mouse. Dev Brain Res 155:147–154

14. **Bouret SG, Draper SJ, Simerly RB** 2004 Formation of projection pathways from the arcuate nucleus of the hypothalamus to hypothalamic regions implicated in the neural control of feeding behavior in mice. J Neurosci 24:2797–2805

15. **Bouret SG, Draper SJ, Simerly RB** 2004 Trophic action of leptin on hypothalamic neurons that regulate feeding. Science 304:108–110

16. **Vickers MH, Gluckman PD, Coveny AH, Hofman PL, Cutfield WS, Gertler A, Breier BH, Harris M** 2005 Neonatal leptin treatment reverses developmental programming. Endocrinology 146:4211–4216

17. **Attig L, Solomon G, Ferezou J, Abdennebi-Najar L, Taouis M, Gertler A, Djiane J** 2008 Early postnatal leptin blockage leads to a long-term leptin resistance and susceptibility to diet-induced obesity in rats. Int J Obes 32:1153–1160

18. **Plagemann A, Harder T, Janert U, Rake A, Rittel F, Rohde W, Dörner G** 1999 Malformations of hypothalamic nuclei in hyperinsulinemic offspring of rats with gestational diabetes. Dev Neurosci 21:58–67

19. **Jawerbaum A, White V** 2010 Animal models in diabetes and pregnancy. Endocr Rev 31:680–701

20. **Tatewaki R, Hashimoto R, Tanigawa K, Furuse K, Tanaka O** 1995 Relationship between associations of NOR and chromosomal anomalies in the abnormal embryos of nonobese diabetic and STZ-diabetic mouse. Biol Neonate 67:132–139

21. **Denroche HC, Levi J, Wideman RD, Sequeira RM, Huynh FK, Covey SD, Kieffer TJ** 2011 Leptin therapy reverses hyperglycemia in mice with streptozotocin-induced diabetes, independent of hepatic leptin signaling. Diabetes 60:1414–1423

22. **Fujikawa T, Chuang JC, Sakata I, Ramadori G, Coppari R** 2010 Leptin therapy improves insulin-deficient type 1 diabetes by CNS-dependent mechanisms in mice. Proc Natl Acad Sci USA 107: 17391–17396

23. **German JP, Wisse BE, Thaler JP, Oh-I S, Sarruf DA, Ogimoto K, Kaiyala KJ, Fischer JD, Matsen ME, Taborsky Jr GJ, Schwartz MW, Morton GJ** 2010 Leptin deficiency causes insulin resistance induced by uncontrolled diabetes. Diabetes 59:1626–1634

24. **Fujii E, Nomoto T** 1988 Effect of streptozotocin administration to pregnant mice on serum glucose, glycosylated hemoglobin and weight of organs of the mother mice and their pups. Jpn J Pharmacol 48:391–394

25. **Bouret SG, Gorski JN, Patterson CM, Chen S, Levin BE, Simerly RB** 2008 Hypothalamic neural projections are permanently disrupted in diet-induced obese rats. Cell Metabolism 7:179–185

26. **Caron E, Sachot C, Prevot V, Bouret SG** 2010 Distribution of leptin-sensitive cells in the postnatal and adult mouse brain. J Comp Neurol 518:459–476

27. **Plagemann A** 2006 Perinatal nutrition and hormone-dependent programming of food intake. Horm Res 65:83–89

28. **Simerly RB** 2005 Wired on hormones: endocrine regulation of hypothalamic development. Curr Opin Neurobiol 15:81–85

29. **Welberg LA, Seckl JR** 2001 Prenatal stress, glucocorticoids and the programming of the brain. J Neuroendocrinol 13:113–128

30. **Plagemann A, Harder T, Melchior K, Rake A, Rohde W, Dörner G** 1999 Elevation of hypothalamic neuropeptide Y-neurons in adult offspring of diabetic mother rats. Neuroreport 10:3211–3216

31. **Franke K, Harder T, Aerts L, Melchior K, Fahrenkrog S, Rodekamp E, Ziska T, Van Assche FA, Dudenhausen JW, Plagemann A** 2005 'Programming' of orexigenic and anorexigenic hypothalamic neu-rons in offspring of treated and untreated diabetic mother rats. Brain Res 1031:276–283

32. **Carmody JS, Wan P, Accil iD, Zeltser LM, Leibel RL** 2011 Respective contributions of maternal insulin resistance and diet to metabolic and hypothalamic phenotypes of progeny. Obesity 19:492–499

33. **Plagemann A, Heidrich I, Götz F, Rohde W, Dörner G** 1992 Lifelong enhanced diabetes susceptibility and obesity after temporary intrahypothalamic hyperinsulinism during brain organization. Exp Clin Endocrinol 99:91–95

34. **Kirk SL, Samuelsson AM, Argenton M, Dhonye H, Kalamatianos T, Poston L, Taylor PD, Coen CW** 2009 Maternal obesity induced by diet in rats permanently influences central processes regulating food intake in offspring. PLoS ONE 4:e5870

35. **Martin-Gronert MS, Ozanne SE** 2005 Programming of appetite and type 2 diabetes. Early Hum Dev 81:981–988

36. **Taylor PD, Poston L** 2007 Developmental programming of obesity in mammals. Exp Physiol 92:287–298

37. **Reusens-Billen B, Remacle C, Daniline J, Hoet JJ** 1984 Cell proliferation in pancreatic islets of rat fetuses and neonates from normal and diabetic mothers. An in vitro and in vivo study. Horm Metab Res 16:565–571

38. **Reusens-Billen B, Remacle C, Hoet JJ** 1989 The development of the fetal rat intestine and its reaction to maternal diabetes. II. Effect of mild and severe maternal diabetes. Diabetes Res Clin Pract 6:213–219

39. **Enzi G, Inelmen EM, Caretta F, Villani F, Zanardo V, DeBiasi F** 1980 Development of adipose tissue in newborns of gestational-diabetic and insulin-dependent diabetic mothers. Diabetes 29:100–104

Go to the ***Translational Research in Endocrinology & Metabolism*** site for a collection of articles from The Endocrine Society journals

www.endojournals.org/trem